===== **ARTICLES** =====

# The Field Emission Properties of Carbon Nanotubes and SiC Whiskers Synthesized over Ni Particles Deposited in Ion Tracks in SiO$_2$

**A. V. Okotrub[a], A. G. Kurenya[a], A. V. Gusel'nikov[a], A. G. Kudashov[a, b],
L. G. Bulusheva[a], A. S. Berdinskii[b], Yu. A. Ivanova[c], D. K. Ivanov[c],
E. A. Strel'tsov[c], D. Fink[d], A. V. Petrov[e], and E. K. Belonogov[f]**

[a] *Nikolaev Institute of Inorganic Chemistry, Siberian Branch, Russian Academy of Sciences,
pr. Akad. Lavrent'eva 3, Novosibirsk, 630090 Russia*

[b] *Novosibirsk State Technical University, pr. Karla Marksa 20, Novosibirsk, 630092 Russia*

[c] *Belarussian State University, ul. Leningradskaya 14, Minsk, 220050 Belarus*

[d] *Helmholtz Centre Berlin for Materials and Energy, str. Glienicker 100, Berlin, D-14109 Germany*

[e] *Scientific Practical Center for Material Sciences, National Academy of Sciences of Belarus, ul. P. Brovki 19, Minsk, 220072 Belarus*

[f] *Voronezh State Technical University, pr. Moskovskii 14, Voronezh, 394026 Russia*

*e-mail: spectrum@che.nsk.su*

Received April 5, 2009; in final form July 3, 2009

**Abstract**—Carbon nanotubes (CNTs) and SiC whiskers are synthesized by the pyrolysis of acetonitrile vapor over Ni nanoparticles deposited in the pores obtained by etching heavy ion tracks in dielectric SiO$_2$ layers on single crystal silicon substrates. The structures obtained are studied by scanning electron microscopy and Raman spectroscopy, and their field emission characteristics are measured. The formation of CNTs or SiC whiskers as a result of catalytic hydrocarbon pyrolysis is found to depend on the occupation of ion tracks by nickel clusters. It is shown that the threshold of electron emission appearance is 1 V/μm for both types of the samples and that differences in the shape of current-voltage characteristics are explained by differences in the electronic structure of CNTs and SiC whiskers.

## INTRODUCTION

The creation of electronic elements based on nanocarbon materials with a number of functional advantages over traditional semiconductor materials seems topical today. In particular, they are expected to operate in a wide range of temperatures, magnetic fields, and under the impact of radiation [1—3]. Therefore, it becomes necessary to develop ways to synthesize carbon nanotubes (CNTs) and to examine the possibilities for creating nanoelectronic devices on their base (field electron emitters, transistors, gas sensors, etc.). Hybrid systems based on silicon and nanocarbon that integrate traditional semiconductor technology with new carbon nanomaterials possessing a unique combination of a number of properties (high strength, electric conductivity, chemical stability, developed surface, and high aspect ratio) are very attractive for creating these devices [2—4]. One task in developing these systems is to achieve the selective growth of CNTs on the surface of silicon plates with the desired density of nanotubes. A low nanotube density in a sample reduces the field screening effect and, hence, increases the efficiency of field cathodes in different devices such as panel displays and x-ray tubes. This task can be solved during the formation of CNTs in ion tracks in silicon oxide on silicon substrates and in sites where heavy ions penetrate the oxidized silicon surface. As was shown in [4—6], the properties of this structure are determined not only by the type of the substrate and the dielectric layer thickness, but also the diameter, depth, shape, and spatial distribution of ion tracks on its surface. Such a procedure helps us create nanopores that can become growth points of CNTs under certain conditions of catalyst deposition in them.

The purpose of this work is to study the growth possibilities for CNTs in ion tracks on the oxidized silicon surface for different pore occupations by metal catalyzing the CNT growth and to analyze the field emission characteristics of the structures obtained.

## EXPERIMENTAL

The main information on the preparation procedure for starting Si/SiO$_2$ structures with ion tracks is given in [4—6]. Plates of KEF-4,5 single crystal silicon with [100] orientation were oxidized in the pure oxygen atmosphere at 1100°C for 10 h. As a result, a layer of SiO$_2$ with a thickness of $0.7 \pm 0.1$ μm formed on the surface of plates. Swift heavy ion ($^{197}$Au$^{26+}$) irradiation with an energy of 350 MeV and fluence of $5 \times 10^8$ cm$^{-2}$
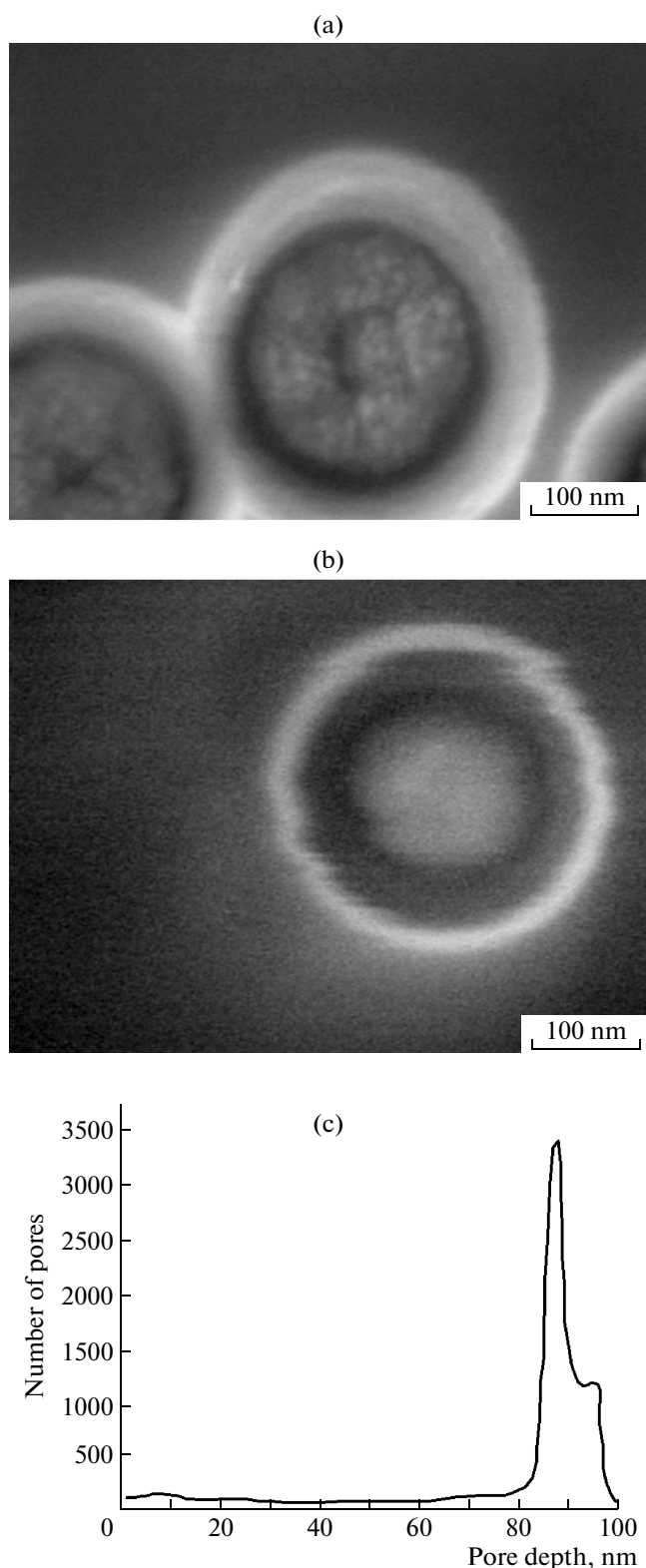
(a)



100 nm

(b)



100 nm

(c)



**Fig. 1.** SEM images of pores on the Si/SiO$_2$ surface, partially (a) and completely (b) filled with nickel. Histogram of the depth distribution of pores filled with nickel (c) derived from AFM data.

performed on a Berlin Ion Beam Exposure and Research Facility (BIBER) apparatus in the ISL Center (Helmholtz Centre for Materials and Energy, Berlin) allowed us to produce regions of local distortions in the oxide layer (regions of increased defectiveness), which are called latent tracks. Latent tracks in the silicon oxide layer after etching in 1.35 wt % hydrofluoric acid solution at a temperature of $20 \pm 1°C$ for 40 min took the form of truncated cones with an average diameter of 150–200 nm and depth of 200 nm. Reaching the silicon surface, the depth corresponded to the SiO$_2$ layer thickness because of its proportional decrease during the simultaneous etching of the tracks.

Nickel electrochemically deposited to nanopores was used as a catalyst for CNT growth. The Si/SiO$_2$ structure with etched ion tracks was placed into an electrochemical cell filled with an electrolyte with a composition of 0.5 m/L H$_3$BO$_3$ + 0.5 m/L NiSO$_4$. The nanopores were filled with metal at a working electrode potential of $-1.2$ V (referring to the saturated silver chloride electrode). One distinguishing feature of the electrochemical deposition method is that it is highly selective, allowing the metal to occupy only the pore region [7, 8].

In this work we present the results of studies of the two most characteristic structures, which differ principally only in the degree of the metal occupation of ion tracks. In one series of samples, the pores are completely filled with nickel; in another they are filled to 30–50% of their depth, which was achieved by varying the deposition time.

Nitrogen-containing CNTs were synthesized by CVD at a temperature of 800°C and atmospheric pressure. Acetonitrile (CH$_3$CN) was used as a source of carbon and nitrogen. Its vapor was introduced into the reactor working zone with an argon flow at a rate of 150 mL/min. The use of these synthesis conditions enables the preparation of CNTs containing 1–4% nitrogen [9, 10].

The surface of substrates before and after CVD synthesis was analyzed using scanning electron microscopy (SEM) on a JEOL JSM-6700F microscope and atomic force microscopy (AFM) on a Solver P47 device. Raman spectra were recorded on a Triplemate spectrometer (SPEX model) with a multichannel detector upon photon excitation with the wavelength $\lambda = 488$ nm.

Current-voltage characteristics (I–V) of field emission of synthesized samples were measured using the device described in [11]. The I–V dependences were recorded in diode mode in a vacuum of $\sim 5 \times 10^{-4}$ Pa at room temperature. The size of samples tested as field cathodes was $5 \times 5$ mm$^2$. Samples on the side of the silicon substrate were stuck to the cathode with conducting double-sided carbon tape. Measurements were performed for two distances from the substrate to the flat molybdenum anode of 500 and

1000 μm. The dependence between the tunnel current value and the electric field was measured by applying a saw-tooth voltage of 1200 V with a frequency of 0.1 Hz.

## RESULTS AND DISCUSSION

Before CVD synthesis, the surface of substrates with tracks partially or completely filled with nickel was analyzed by SEM and AFM (Fig. 1). After etching the ion tracks, pores on the $SiO_2$ surface had the form of regular circles with a diameter of 150−200 nm; the characteristic distance between the pores was ~1 μm. The image in Fig. 1a shows that the electrochemical deposition of nickel with the partial occupation of the pore proceeds with the formation of crystallites ~50 nm in size that relatively weakly contact each other. When the pore is completely filled, no features in the surface structure of the nickel particle were revealed (Fig. 1b). Nickel deposition in the pores is controlled by inspecting the occupation quite often. Fig. 1c displays a histogram based on the processing results of AFM data. It confirms that the distance from a nickel particle to the $SiO_2$ surface has a narrow distribution of filled pores. Hence, in the electrochemical process, nickel fills the pores at about the same depth.

A study of samples synthesized by CVD on the surface of substrates shows that the formation of carbon-containing structures on nickel particles proceeds differently for samples with varying metal occupation of pores. On substrates with pores partially filled with nickel, a layer of nanotubes with a length of ~10 μm and diameter of ~50 nm forms (Fig. 2a). Electron microscopic analysis of the growth surface reveals that, as a rule, each pore initiates the growth of one nanotube. However, almost in 20% cases, 2 or 3 nanotubes grow from one pore. Moreover, about 10% of the pores remained inactive in the synthesis. The CNTs obtained are not straight but represent twisted structures interlaced with each other. This result indicates the tip mechanism of nanotube growth when a metallic nanoparticle catalyst breaks away from the sample surface. Because the nanotubes grow in the gas phase, it causes them to bend to one or another side relative to the $SiO_2$ surface. Our previous use of iron nanoparticles deposited on oxidized silicon substrates resulted in the root growth of CNTs and, hence, to the mutual orientation of nanotubes perpendicularly to the substrate surface [12]. In order to confirm the tip growth of CNTs, we synthesized a sample by CVD for 15 min. As a result of the synthesis, short CNTs with a length of ~2 μm and diameter of ~50 nm formed on the substrate surface (Fig. 2b). A small length of CNTs allowed us to take the image from the pore to the nanotube end on which roundish agglomerates are seen. These agglomerates at the CNT end are nickel nanoparticles, because at the microscope electron beam energy of 15 keV the metallic particles under a thin carbon layer are observed as bright light spots. The
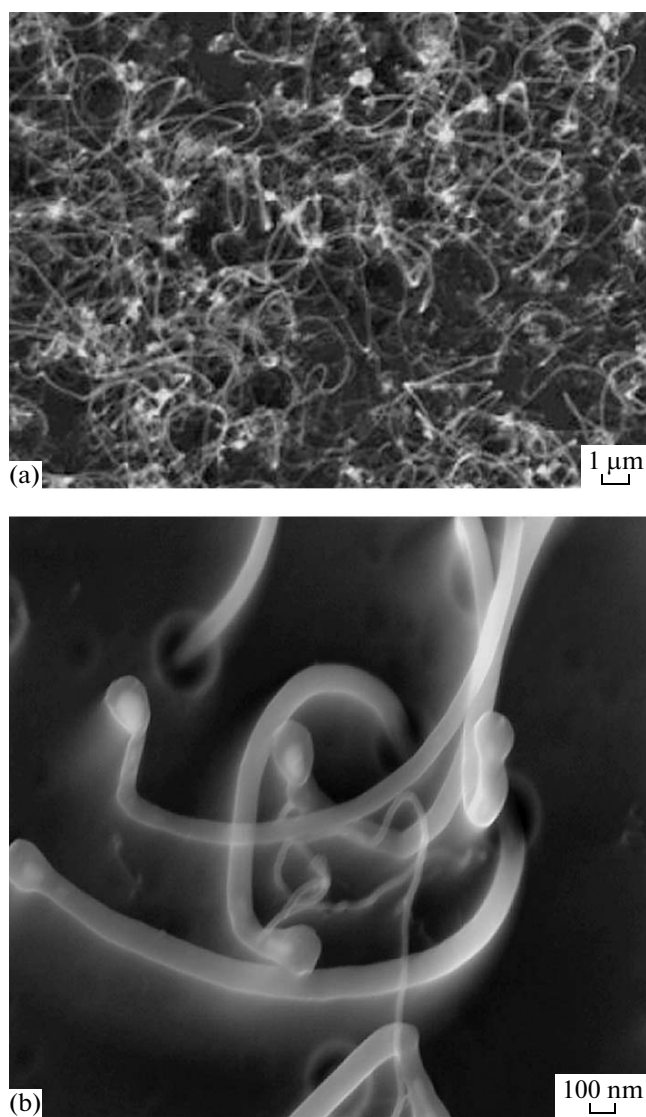


(a)  1 μm

(b)  100 nm

**Fig. 2.** SEM image of CNTs formed on the $Si/SiO_2$ substrate with pores partially filled with nickel after CVD synthesis for 1 h (a) and 15 min (b).

characteristic size of metal catalyst nanoparticles is ~50 nm, which corresponds to the size of separate nickel crystallites inside the pore. Due to acetonitrile pyrolysis, one of the nickel particles (possibly the central) without any contact with silicon oxide breaks away from the substrate, which results in CNT growth. The detachment of two metal clusters induces the simultaneous growth of two nanotubes from one pore.

We can see another picture when, in the CVD process, the $Si/SiO_2$ substrates, whose pores are completely filled with nickel, are used. Synthesis carried out for 1 h led to the formation of straight and short nanostructures on the surface of substrates (Fig. 3a). These structures strongly differ from those obtained under the same conditions of CNT synthesis (Fig. 2a). High magnification allows us to see that the nano-
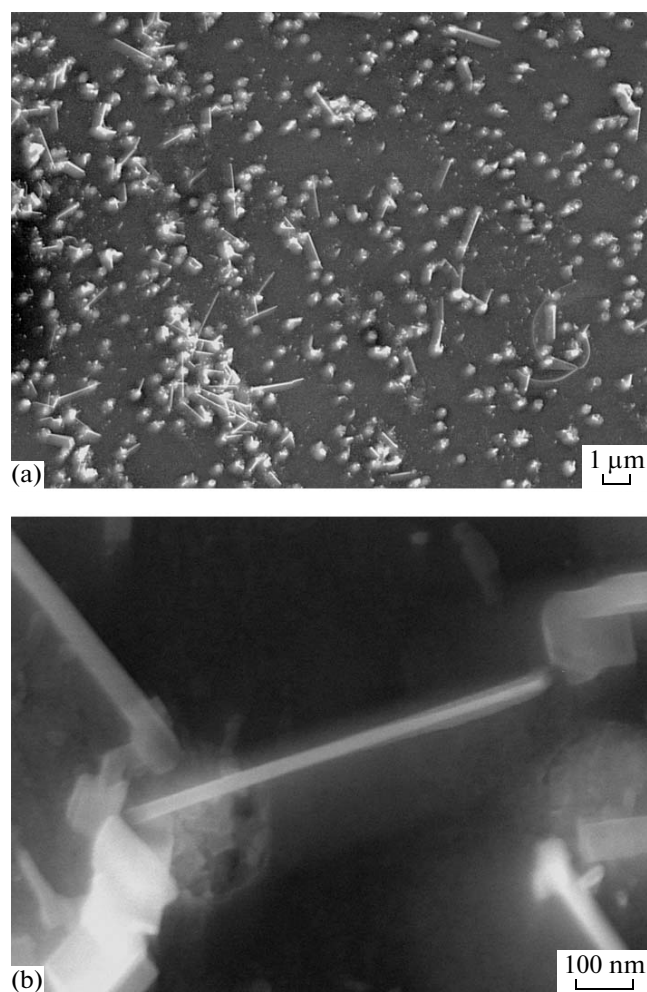
**Fig. 3.** SEM images of SiC whiskers formed on the Si/SiO$_2$ substrate with pores completely filled with nickel after CVD synthesis for 1 h: (a) lower magnification and (b) higher magnification.

structures obtained are single crystal whiskers with a submicron length and characteristic lateral size of 10 nm (Fig. 3b). It is known that, under certain conditions, nickel nanoparticles can catalyze the synthesis of SiC whiskers [13]. One may assume that a nickel particle which is tightly bound to the pore surface and has a homogeneous crystal structure cannot serve as a catalyst of the tip growth of CNTs. The formation of whiskers can be associated with both the carbon saturation of nickel particles due to acetonitrile pyrolysis and the partial dissolution of silicon in the nickel particle. The heterogeneous process of silicon introduction into the nickel particle may be why thin and relatively short SiC whiskers form.

The preferential formation of whiskers at the pore boundary (Fig. 3b) suggests that the limiting stage of their growth is silicon diffusion along the nickel particle boundary.

Synthesis products formed on the surface of Si/SiO$_2$/Ni substrates with different occupations of pores were studied by Raman spectroscopy. In the range under analysis, three frequency regions are typical of the silicon-carbon system. Frequencies in the ranges of 100 to 700 and of 700 to 1100 cm$^{-1}$ are traditionally assigned to the vibrations of Si-Si and Si-C bonds respectively, whereas the vibrations of carbon atoms manifest themselves in the range from 1200 to 1700 cm$^{-1}$. In the spectrum of a sample with incomplete nickel occupation, the line at 520 cm$^{-1}$, which is related to silicon vibrations, is weak (Fig. 4). The most intense lines at 1367 cm$^{-1}$ (D mode) and 1582 cm$^{-1}$ (G mode) correspond to the vibrations of the carbon that forms CNT layers [14]. This spectrum is typical of multilayer nanotubes obtained by CVD, and the relative intensity of D and G modes is used as a parameter characterizing the defectiveness of the graphite network [14]. In the spectrum of a sample with pores completely filled with nickel, the line related to silicon vibrations dominates, which is due to the low concentration of whiskers on the substrate surface. The formation of SiC nanostructures is confirmed by the presence of phonon modes at 815 and 966 cm$^{-1}$ in the Raman spectrum [15, 16].

Figure 5 depicts I−V dependences of the field emission of both types of samples. Despite the fact that in the sample containing CNTs the tubes are not oriented perpendicularly to the surface, the cathode shows quite low values of the field voltage at which the emission current appears (Fig. 5a). Low threshold fields are provided by two parameters, namely the rather large distances between the nanotubes reducing the screening effect [17] and the presence of nitrogen in the CNT structure [18]. The sample that mainly consists of SiC whiskers demonstrated quite good field emission properties (Fig. 5b). Silicon carbide is a semiconductor; however, in the case of whiskers, it can have fairly good surface conductivity. Indeed, the emission current value measured in this case is only four times lower than that for the sample consisting of CNTs. A comparison between the I−V dependences of samples at interelectrode distances of 500 and 1000 μm reveals that the threshold field value increases at a shorter distance. The reason for the dependence of the threshold field on the interelectrode distance is a change in the field enhancement factor [19]. The maximum value of the enhancement factor is determined by the aspect ratio of the nanotube length to its diameter for single CNTs or it has a more complicated dependence on the array of nanotubes because of their mutual screening [20]. The characteristics obtained at large distances, when the dependence of the threshold field on the interelectrode distance reaches its maximum and approaches saturation, are most adequate for describing the field emission processes. The threshold field values obtained are almost similar for both samples. It may be suggested that the small value
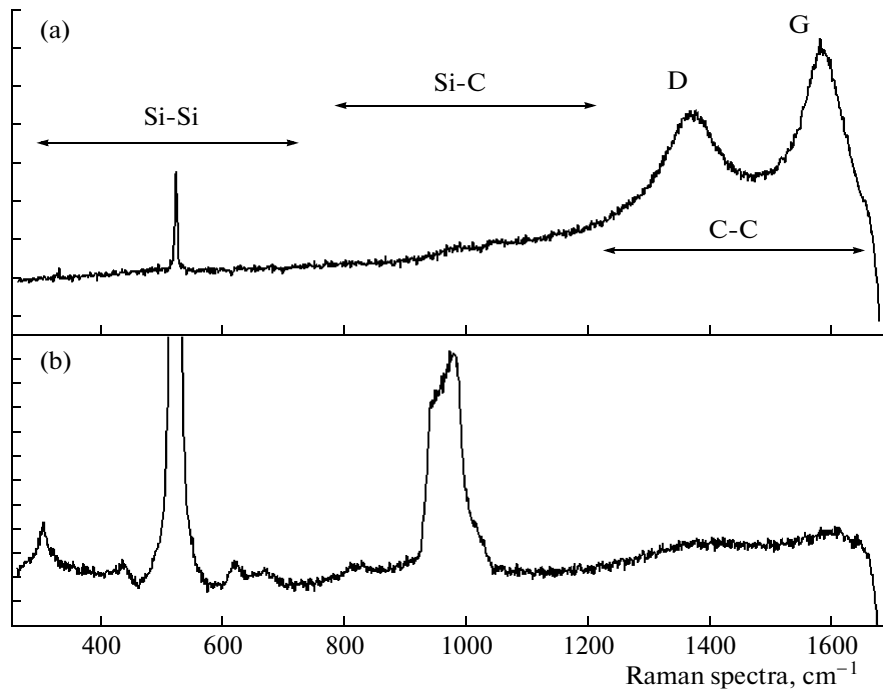
**Fig. 4.** Raman spectra of synthesized samples: (a) CNTs and (b) Si C whiskers.
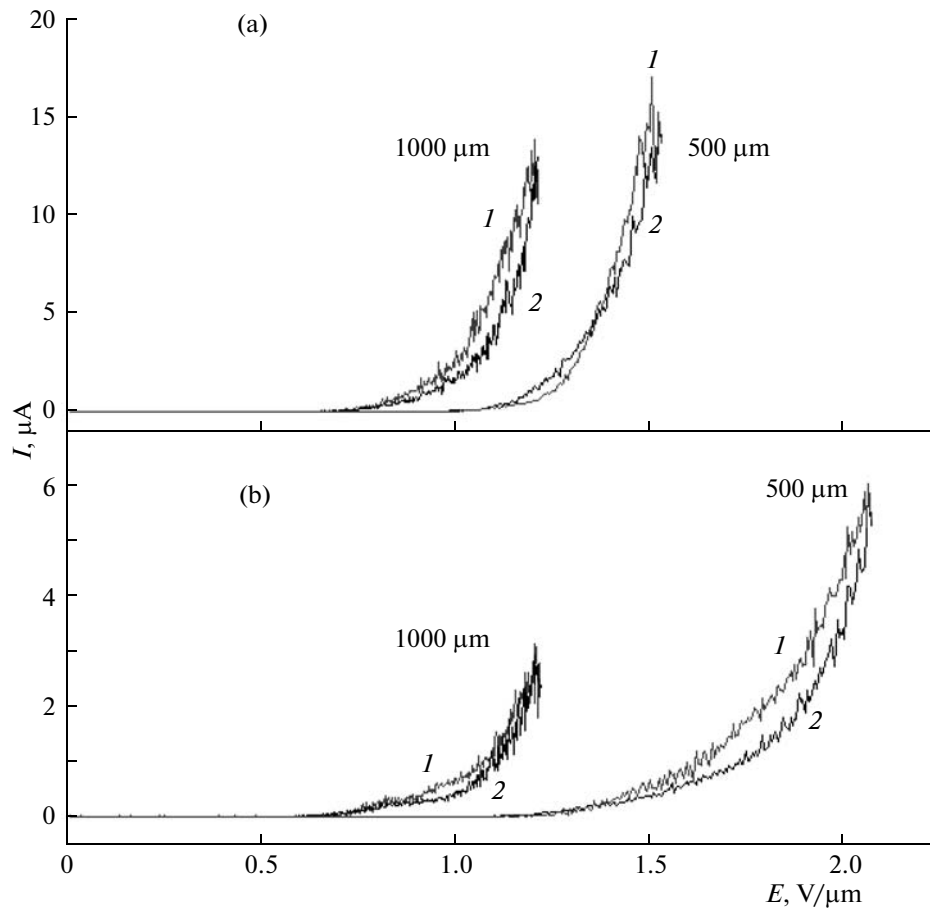


**Fig. 5.** I−V dependences of the field emission current for the samples of (a) CNTs and (b) SiC whiskers measured at interelectrode distances of 500 and 1000 μm. (*1*) and (*2*) correspond to measurements with increasing and decreasing saw-tooth voltage.

of the aspect ratio for SiC whiskers (when compared to nanotubes) is compensated for by the somewhat smaller electron work function from silicon carbide.

I−V dependences of the field emission measured on ascending and descending branches of the sawtooth voltage demonstrated the occurrence of hysteresis even at a frequency of 0.1 Hz. The appearance of hysteresis can be caused by the desorption of residual gases from the surface of CNTs [21]; the molecules with dipole moment ($H_2O$, CO, etc.) are most often related to them [22]. The occurrence of hysteresis in the form of a figure eight observed for the sample with CNTs at a distance of 500 μm indicates the presence of at least two mechanisms of molecular desorption. Indeed, thermoionic processes accompany the appearance of the field emission current. Near the threshold of the current appearance, electrons can tunnel from one end of the nanotube to the adsorbed molecule, which results in the emergence of a negative ion current [23]. At a higher value of the applied voltage, the nanotube is ohmically heated because of the current flow through it, which induces gas desorption from the nanotube surface. Each molecule adsorbed on the CNT surface or SiC whisker modifies their electronic structure; this is accompanied by electron density redistribution, which changes the nanoparticle working function.

We should note the differences in I−V dependences of the samples studied. They may be due to the features of the electronic structure of SiC whiskers and CNTs. In particular, I−V curves of whiskers start with exponential growth; then they have a weak bend in the fields of 0.8 V/μm, and exponential growth is observed again, which may be caused by the heterogeneous size distribution of whiskers in the sample. The hysteresis of emission on the whiskers is much smaller than that on the nanotubes, which may give evidence of a difference in the chemical interaction between adsorbate molecules and nanostructures, as well as of the different effect that these interactions have on the electronic properties of the objects under study.

## CONCLUSIONS

It is shown that Si/SiO₂ structures with ion tracks in the dielectric filled with nickel can be used to synthesize CNTs and single crystal SiC whiskers with a controlled density of nanostructures in the sample. It is found that, in order to synthesize CNTs, conditions are required for the tip mechanism of growth. Here the catalytic synthesis of nanotubes from pores is possible at their incomplete occupation by the metal-catalyst. Otherwise, SiC whiskers grow by the root mechanism. The high efficiency of field emission of the samples obtained, whose emission threshold is less than 1 V/μm, is demonstrated. Differences in the form of I−V curves of samples may be due to the different work functions of CNTs and SiC whiskers, as well as the different

effects that adsorbed gases have on the electronic state of these nanostructures.

## REFERENCES

1. J.-M. Bonard, H. Kind, T. Stöckli, and L.-O. Nilson, Solid-State Electron. **45**, 893 (2001).
2. Y.-M. Lin, J. Appenzeller, J. Knoch, and P. Avouris, IEEE Trans. Nanotechnol. **4**, 481 (2005).
3. Y.-T. Jang, C.-H. Choi, B.-K. Ju, J.-H. Ahn, and Y.-H. Lee, Thin Solid Films **436**, 298−302 (2003).
4. A. S. Berdinsky, P. S. Alegaonkar, H. C. Lee, J. S. Jung, J. H. Han, J. B. Yoo, D. Fink, and L. T. Chadderton, NANO: Brief Rep. Rev. **2** (1), 59 (2007).
5. D. Fink, A. V. Petrov, K. Hoppe, W. R. Fahrner, R. M. Papaleo, A. S. Berdinsky, A. Chandra, A. Chemseddine, A. Zrineh, A. Biswas, F. Faupel, and L. T. Chadderton, Nucl. Instrum. Methods Phys. Res., Sect. B **218**, 355 (2004).
6. K. Hoppe, W. R. Fahrner, D. Fink, S. Dhamodoran, A. Petrov, A. Chandra, A. Saad, F. Faupel, V. S. K. Chakravadhanula, and V. Zaporotchenko, Nucl. Instrum. Methods Phys. Res., Sect. B **266** (8), 1642 (2008).
7. D. K. Ivanov, E. A. Streltsov, A. K. Fedotov, A. V. Mazanik, D. Fink, and A. Petrov, Thin Solid Films **490**, 154 (2005).
8. Yu. A. Ivanova, D. K. [!]Ivanou, A. K. Fedotov, E. A. Streltsov, S. E. Demyanov, A. V. Petrov, E. Yu. Kaniukov and D. Fink, J. Mater. Sci. **42**, 9163 (2007).
9. C. P. Ewels and M. Glerup, J. Nanosci. Nanotechnol. **5**, 1 (2005).
10. L. G. Bulusheva, A. V. Okotrub, I. A. Kinloch, I. P. Asanov, A. G. Kurenya, A. G. Kudashov, X. Chen, and H. Song, Phys. Status Solidi B **245** (10), 1971 (2008).
11. A. V. Okotrub, L. G. Bulusheva, and A. V. Gusel'nikov, Zh. Eksp. Teor. Fiz. **126** (6), 1425 (2004) [JETP [!]**99** (6), 1244 (2004)].
12. A. V. Okotrub, L. G. Bulusheva, A. G. Kudashov, V. V. Belavin and S. V. Komogortsev, Ross. Nanotekhnol. **3** (3−4), 28 (2008) [Nanotechnol. Russ. **3** (3−4), 191 (2008)].
13. V. L. Kuznetsov, A. N. Usoltseva, and I. N. Mazov, Fullerenes, Nanotubes, Carbon Nanostruct. **13**, 121 (2005).
14. R. A. Afre, T. Soga, and T. Jimbo, Chem. Phys. Lett. **414**, 6 (2005).

15. M. Makowska-Janusik, A. Kassiba, and J. Bouclé, J. Phys.: Condens. Matter **17**, 5101 (2005).

16. W. Shi, Y. Zheng, H. Peng, N. Wang, C. S. Lee, and S.-T. Lee, J. Am. Ceram. Soc. **83** (12), 3228 (2000).

17. W. I. Milne, K. B. K. Teo, G. A. J. Amaratundra, P. Legagneux, L. Gangloff, J.-P. Schnell, V. Semet, V. Thien Binh, and O. Groening, J. Mater. Chem. **14**, 933 (2004).

18. A. V. Okotrub, L. G. Bulusheva, V. V. Belavin, A. G. Kudashov, A. V. Gusel'nikov, and S. L. Molodtsov, Fullerenes, Nanotubes, and Carbon Nanostruct. **14**, 151 (2006).

19. R. C. Smith, D. C. Cox, and S. R. P. Silva, Appl. Phys. Lett. **87**, 103 112 (2005).

20. D. Kim, J. E. Bourée, and S. Y. Kim, Appl. Phys. A: Mater. Sci. Process. **83**, 111 (2006).

21. C. Liu, C. Cutshaw, and Y. Tzeng, in *Proceedings of the Sixth Applied Diamond Conference/Second Frontier Carbon Technology Conference (ADC/FCT 2001), Auburn, AL, United States, 2001* (Auburn, 2001), p. 72.

22. W. I. Milne, K. B. K. Teo, S. B. Lansley, et al., in *Molecular Nanostructures*, Ed. by H. Kuzmany, J. Fink, M. Mehring, and S. Roth, in *AIP Conference Proceedings* (American Institute of Physics, Melville, New York, United States, 2003), Vol. 685, p. 605.

23. A. V. Okotrub, A. V. Gusel'nikov, A. G. Kudashov, I. V. Bugakov, and L. G. Bulusheva, Phys. Status Solidi B **243** (13), 3510 (2006).